Materials Science and Engineering C 54 (2015) 94–100

Contents lists available at ScienceDirect

Materials Science and Engineering C

journal homepage: www.elsevier.com/locate/msec

Original article

Revival of pure titanium for dynamically loaded porous implants using additive manufacturing

Ruben Wauthle [a,b,*], Seyed Mohammad Ahmadi [c], Saber Amin Yavari [c], Michiel Mulier [d], Amir Abbas Zadpoor [c], Harrie Weinans [c,e], Jan Van Humbeeck [f], Jean-Pierre Kruth [a], Jan Schrooten [f,g]

[a] KU Leuven, Department of Mechanical Engineering, Section Production Engineering, Machine Design and Automation (PMA), Celestijnenlaan 300B, 3001 Leuven, Belgium
[b] 3D Systems - LayerWise NV, Grauwmeer 14, 3001 Leuven, Belgium
[c] Faculty of Mechanical, Maritime, and Materials Engineering, Delft University of Technology (TU Delft), Mekelweg 2, 2628 CD, Delft, The Netherlands
[d] KU Leuven, Department of Orthopaedics, Weligerveld 1, 3212 Pellenberg, Belgium
[e] Department of Orthopedics & department of Rheumatology, UMC Utrecht, Heidelberglaan 100, 3584 CX, Utrecht, The Netherlands
[f] KU Leuven, Department of Materials Engineering, Kasteelpark Arenberg 44, PB 2450, 3001 Leuven, Belgium
[g] KU Leuven, Prometheus, Division of Skeletal Tissue Engineering, PB 813, O&N1, Herestraat 49, 3000 Leuven, Belgium

ARTICLE INFO

Article history:
Received 17 November 2014
Received in revised form 17 March 2015
Accepted 2 May 2015
Available online 5 May 2015

Keywords:
Additive manufacturing
Selective laser melting
Titanium
Fatigue
Porous biomaterials

ABSTRACT

Additive manufacturing techniques are getting more and more established as reliable methods for producing porous metal implants thanks to the almost full geometrical and mechanical control of the designed porous biomaterial. Today, Ti6Al4V ELI is still the most widely used material for porous implants, and none or little interest goes to pure titanium for use in orthopedic or load-bearing implants. Given the special mechanical behavior of cellular structures and the material properties inherent to the additive manufacturing of metals, the aim of this study is to investigate the properties of selective laser melted pure unalloyed titanium porous structures. Therefore, the static and dynamic compressive properties of pure titanium structures are determined and compared to previously reported results for identical structures made from Ti6Al4V ELI and tantalum. The results show that porous Ti6Al4V ELI still remains the strongest material for statically loaded applications, whereas pure titanium has a mechanical behavior similar to tantalum and is the material of choice for cyclically loaded porous implants. These findings are considered to be important for future implant developments since it announces a potential revival of the use of pure titanium for additively manufactured porous implants.

1. Introduction

Porous metal structures in orthopedics were first reported in the late sixties, and ever since then the interest has only increased [1–3]. The reasons for this trend in reconstructive surgery are obvious: coming from solid metal implants with high strength and stiffness, porous metals are optimal for uncemented use since they allow for bone ingrowth through the open porosities, have an improved fixation thanks to the high roughness and corresponding coefficient of friction and have in addition a lower stiffness and thus avoid stress-shielding [4]. Today, one of the most well-known porous metal bone replacement structures is *Trabecular Metal™* (Zimmer, Warsaw, IN, USA), which is a highly porous carbon matrix coated with tantalum (Ta) [1,5–9]. But due to the high density and high cost of Ta and its difficulty to process, most orthopedic device manufacturers choose to use porous biomaterials based on titanium or titanium alloys [2,3,10]. These titanium porous structures are usually manufactured using conventional techniques such as furnace sintering, plasma spraying, lost wax casting and vapor deposition [10–13]. Recently, additive manufacturing (AM) techniques such as selective laser melting (SLM, [14]) and electron beam melting (EBM) are breaking new ground in implant manufacturing and more specifically in the manufacturing of porous metal bone replacement structures. AM allows for almost full design freedom, giving the possibility to manufacture regular open porous structures with high repeatability and thus full control over both geometrical and mechanical properties. The design freedom and reproducibility are important features when there is a need for implant performance simulations and outcome predictions [15,16]. Also, using AM has the advantage to manufacture implants with both porous and solid sections in one step (monolithic design), with less material consumption since the non-used powder can be recycled for future use, when the chemical composition is still fulfilling the required specifications and when the recycling process is free from contamination. Finally, materials like Ta that are difficult to process conventionally, could be also processed using AM, creating a whole range of new opportunities [17].

In the current study, the SLM technology was used to manufacture porous structures from commercially pure (CP) grade 1 titanium. Previous studies mostly dealt with porous structures in Ti6Al4V (grade 5 or

* Corresponding author at: 3D Systems – LayerWise NV, Grauwmeer 14, 3001 Leuven, Belgium.
E-mail address: ruben.wauthle@3dsystems.com (R. Wauthle).

http://dx.doi.org/10.1016/j.msec.2015.05.001
0928-4931/

grade 23), either using SLM [15,16,18–30] or EBM [13,31–36]. This biocompatible titanium alloy is the material of choice for load-bearing applications since it has a high strength to weight ratio. Commercially pure titanium (CP Ti), on the other hand, has a lower strength and therefore its use is often limited to non-load bearing applications like craniomaxillo-facial implants [37]. A general overview of these mechanical properties of different grades of titanium and Ta can be found in Table 1.

Also, only few publications about additively manufactured CP Ti are available, all of them covering SLM of CP Ti grade 2 [41–45] and none were found that deal with CP Ti grade 1. Nevertheless, the use of CP Ti has some major advantages over alloyed titanium that can potentially bring additively manufactured CP Ti back in the scope of medical device manufacturers. First of all, CP Ti has the advantage of having no potential hazardous or toxic alloying components such as V or Al [1]. Secondly, the high ductility that provides CP Ti with the sometimes necessary deformability in certain applications like e.g. bone plates, could be an interesting property of porous metals that could be deformed intra operatively to the patient specific bone defect. And finally, in a previous study on porous Ta structures, the ductile behavior of the Ta material led to a very high fatigue strength compared to similar Ti6Al4V ELI structures and a preferential load transfer and bone ingrowth in an animal study [17]. It was proposed that the mechanical behavior of the porous Ta including its high ductility was partly responsible for the excellent *in vivo* performance of Ta. Therefore, the aim of this study is to investigate whether CP Titanium can have a revival in orthopedics as a raw material for SLM processed porous implants. This is the first study that presents and discusses the mechanical properties of additively manufactured porous structures made of CP Ti grade 1 and compares them with those of additively manufactured Ti6Al4V ELI and Ta structures. This could be useful for facilitating proper selection of the most appropriate material for the envisioned implant application.

2. Materials and Methods

The materials and methods section describes the details of the new porous CP grade 1 Ti samples, manufactured and analyzed in the current study. The properties of identical porous structures made from Ti6Al4V ELI and Ta to which the CP Ti samples will be compared were published elsewhere, unless otherwise implied [17,23].

2.1. Materials and manufacturing

Porous CP Ti grade 1 structures were manufactured from CP Ti grade 1 powder using the selective laser melting technology (3D Systems - Layerwise NV, Leuven, Belgium). The details of the laser processing method were similar to the ones presented in previous studies [19–21,23]. The unit cell used as the micro-architecture of these porous structures was in all cases dodecahedron, in four different porosities as seen on Fig. 1. This specific unit cell, pore and strut sizes were chosen in order to compare the results with those of a previous study that used identical dodecahedron structures made by SLM out of Ti6Al4V ELI powder [23]. The used nomenclature in Fig. 1 refers to the theoretical strut and pore size; e.g. Ti 120 – 500 has a theoretical strut size of 120 μm and pore size of 500 μm. In this work, spherical commercially pure grade 1 Ti powder (chemical composition according to ASTM F67, further referred to as CP Ti) with particle size ranging from 10 μm to 45 μm was used. The production was performed in an inert atmosphere and the samples were built on top of a solid Ti substrate. After production, the samples were removed from the substrate using wire electro discharge machining (EDM). Cylindrical porous specimens with a diameter of 10 mm and height of 15 mm were manufactured for morphological analysis, static and dynamic mechanical testing. The chemical composition of the porous specimens after SLM manufacturing was measured using IGA (Interstitial Gas Analysis) and ICP-OES (Inductively Coupled Plasma Optical Emission Spectrometry). With measured concentrations of C (0.0075 % wt), N (0.0100 % wt), O (0.1600 % wt), H (0.0036 % wt) and Fe (0.040 % wt), the specifications of ASTM F67 for CP Ti grade 1 are fulfilled.

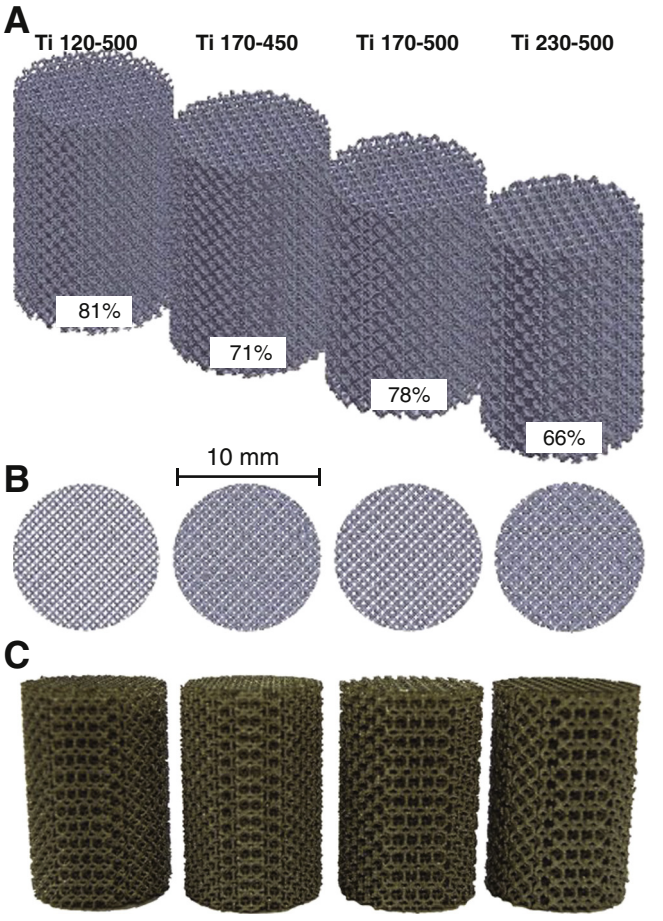

Fig. 1. Additively manufactured porous CP Ti structures: 3D CAD visual representation of the four different structures in isometric (A) and top (B) view and a picture after manufacturing (C).

Table 1
Literature values of the density and mechanical properties of standard annealed wrought titanium grades [38] and tantalum [39,40]: The density, yield strength (YS), the ultimate tensile strength (UTS), Young's modulus (E) and the elongation (e). Fatigue data are taken from [1].

Material	Density [g/cm^3]	YS [MPa]	UTS [MPa]	E [GPa]	e [%]	Fatigue [MPa]
CP Ti grade 1	4.51	170-241	240-331	103	30	270
CP Ti grade 2	4.51	280-345	340-434	103	28	330
CP Ti grade 3	4.51	380-448	450-517	103	25	350
CP Ti grade 4	4.51	480-586	550-662	104	20	376
Ti6Al4V grade 5	4.43	830-924	900-993	114	14	500
Ti6Al4V ELI grade 23	4.43	760-827	830-896	114	15	n.a.
Tantalum	16.6	165-220	200-390	186	20-50	n.a.

2.2. Morphological analysis

Overall open porosity was measured using dry weighing and Archimedes measurements on five different cylindrical samples prior to being used for mechanical testing. Dry weighing occurred under normal atmosphere conditions and overall porosity was calculated by dividing the actual weight by the theoretical weight of the macro volume using

a theoretical density of 4.507 g/cm^3 for pure Ti [39]. Archimedes measurements are based on a combination of dry weighing and weighing in pure ethanol. The absolute density (ρ_{abs}) of each porous specimen was calculated using the equation:

$$\rho_{abs} = \frac{m_{air}(\rho_{ethanol} - 0.0012)}{m_{air} - m_{ethanol}} + 0.0012$$

Where m_{air} is the weight of the porous specimen in air, $m_{ethanol}$ the weight of the porous specimen while immersed in ethanol and $\rho_{ethanol}$ is the density of ethanol. Dividing the weight in air by the absolute density resulted in the actual volume, while the overall porosity was then calculated by dividing the actual volume by the macro volume. All weighing measurements were performed on an OHAUS Pioneer balance.

2.3. Mechanical testing

2.3.1. Static mechanical testing

Static mechanical testing of five cylindrical samples of each of the four series of porous structures was carried out in accordance with the standard ISO 13314 [46]. All tests were done using an INSTRON 5985 mechanical testing machine (30 kN load cell) by applying a constant deformation rate of 1.8 mm/min. Each static compression test resulted in a stress–strain curve (Fig. 3) for which the following values were calculated: plateau stress (σ_{pl}) as the arithmetical mean of the stresses between 20% and 40% compressive strain, plateau end stress (σ_{130}) and strain (e_{ple}) as the point in the stress–strain curve at which the stress is 1.3 times the plateau stress, the quasi-elastic gradient (E) as gradient of the straight line determined within the linear deformation region at the beginning of the compressive stress–strain curve and the yield strength (σ_y) as the compressive 0.2% offset stress. In this context, the quasi-elastic gradient is closest to the concept of stiffness, which is used for solid materials. In order to facilitate understanding and comparison between the results of this study and those of similar studies on solid and porous materials, the quasi-elastic gradient will be referred to as stiffness. Nevertheless, the exact definitions presented above should be kept in mind when interpreting the data. In the previous study on Ti6Al4V ELI porous structures, it was assumed that the plateau stress was close to the concept of yield stress [23], and this is confirmed by re-calculating the yield stress according the 0.2% offset stress

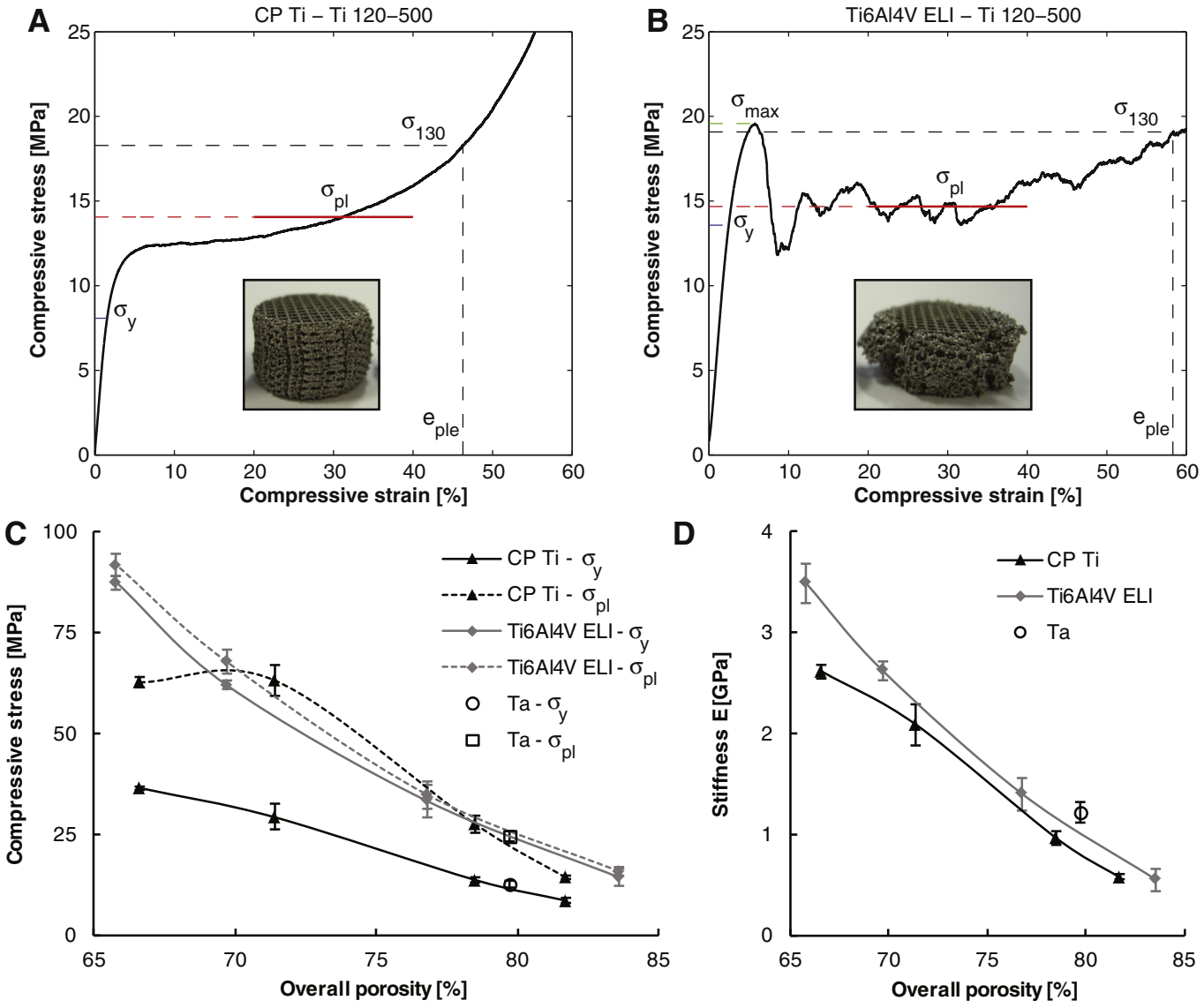

Fig. 2. Static mechanical properties of open porous SLM processed titanium and tantalum structures: representative compressive stress–strain curve and graphical representation of the calculated values σ_y, σ_{pl}, σ_{130}, e_{ple} for a Ti 120–500 structure in CP Ti (A) and Ti6Al4V ELI (B), both including a picture of a sample after compression testing; and a comparison between the yield strength and plateau stress (C) and stiffness (D) for all three materials versus the actual measured open porosity of each structure.

explained above (solid and dashed grey lines in Fig. 2 C). For three out of four data points, there is no significant difference between the yield stress and the plateau stress for Ti6Al4V ELI porous structures, meaning that the assumptions were valid. However, for CP Ti porous structures, there is a significant difference between the yield stress and the plateau stress, and therefore both values were calculated and analyzed separately.

2.3.2. Dynamic mechanical testing

Compression-compression fatigue tests were carried out on an identical set-up as reported before [23] using a hydraulic test frame (MTS, Minneapolis, US) with a 25 kN load cell. The loading frequency was fixed at 15 Hz (sinusoidal wave shape) and a constant load ratio, $R = 0.1$ was used (load ratio is the ratio of the minimum load to the maximum load applied during the cycle). Ten different values of maximum force were chosen for every porous structure (except one, for which only 7 values were tested), resulting in applied stress levels between 0.45 σ_y and 0.8 σ_y. Two samples were tested for each stress level with 20 samples in total for series Ti 120–500, Ti 170–500 and Ti 230–500 and 14 samples for series Ti 170–450 (see Fig. 1 and Table 2 for details on the series nomenclature). The samples were considered to have failed once they lost +90% of their stiffness. The S-N curves of the four tested porous structures were established by plotting both absolute and normalized values of stress versus number of cycles to failure for all tested samples. In case of normalized S-N curves, a power law was fitted to all data points of the normalized S-N curves.

3. Results

3.1. Morphological properties

The measured values for the overall porosity by dry weighing and Archimedes measurements are summarized in Table 2. A high repeatability in terms of overall porosity (<1%) and a high density of the struts (>98%) was achieved, which is of importance for reproducibility of the mechanical properties.

3.2. Mechanical properties

The results of the static compression tests are summarized in Table 3. Due to the ductile behavior of the porous CP Ti material, no maximum compressive stress (σ_{max}) and strain at maximum compressive stress (e_{max}) could be registered. Fig. 2 A shows a representative stress–strain curve and the ductile behavior of the porous CP Ti Ti 120–500 structure during static compression testing, including a graphical representation of all calculated properties. The actual values of the static mechanical properties are summarized in Table 3 and are visually presented and compared to Ti6Al4V ELI and Ta in Fig. 2 C and D, in which the actual open porosity of each porous structure is taken into account. For the Ta values, σ_{pl} was recalculated for the 20-40% strain interval instead of the previously reported 20-30% strain interval.

The dynamic compression test results are shown through S-N curves in Fig. 3 A for absolute and in Fig. 3 B for normalized stress values obtained by compression-compression fatigue testing, including the power law for the normalized S-N curves of Ti6Al4V ELI and Ta structures as reported previously [17,23]. Power laws were fitted to the normalized data points of all four series and to all series together and are represented in Table 4. The coefficient of determination was very high for all fitted power laws, but it should be noted that the series Ti 170–450 and the combined data have a lower coefficient of determination. When multiplying these power laws by the yield strength of each series for both materials, this results in power laws for the absolute stress values as shown in Fig. 3 C. The point where the same series in the two materials intersect is marked with an 'X'. It should be noted that Fig. 3 C assumes that each of the four series in CP Ti are completely identical to the corresponding series in Ti6Al4V ELI, while in fact there are minor differences in overall open porosities between them, which should be kept in mind while interpreting this figure. In conclusion, Fig. 3 D shows the fatigue strength S_f after 10^6 cycles, for CP Ti based on an extrapolation of the fitted power laws in Table 4, for Ti6Al4V ELI based on the estimated fatigue strength of 0.12 σ_y in [23], taking into account the actual overall porosity for both materials and for all four series, and finally for Ta based on the determined fatigue strength of 7.35 MPa (or 0.57 σ_y) for only one porosity mentioned in [17].

Table 2
The geometrical/physical properties of the four different series of porous CP Ti samples tested in the current study.

Series	Ti 120-500	Ti 170-450	Ti 170-500	Ti 230-500
Porosity,dry weighing [%]	81.7 ± 0.2	71.4 ± 0.6	78.5 ± 0.3	66.7 ± 0.4
Porosity,Archimedes [%]	81.6 ± 0.2	71.1 ± 0.6	78.4 ± 0.4	66.0 ± 0.6
Strut density, Archimedes [%]	99.8 ± 0.2	99.2 ± 0.1	99.5 ± 0.3	98.0 ± 1.1
Pore size,nominal [μm]	500	450	500	500
Strut size,nominal [μm]	120	170	170	230

Table 3
The static mechanical properties of the four different series of porous CP Ti samples tested according to ISO 13314.

Series	σ_y [MPa]	σ_{pl} [MPa]	σ_{130} [MPa]	e_{ple} [%]	E [GPa]
Ti 120-500	8.6 ± 0.3	14.3 ± 0.2	18.6 ± 0.3	46.3 ± 0.4	0.58 ± 0.02
Ti 170-450	29.2 ± 2.3	63.2 ± 3.8	82.3 ± 5.2	40.3 ± 0.5	2.08 ± 0.14
Ti 170-500	13.7 ± 0.4	27.6 ± 2.2	36.3 ± 3.4	41.4 ± 2.3	0.96 ± 0.05
Ti 230-500	36.5 ± 0.4	62.7 ± 1.4	81.5 ± 1.9	42.4 ± 0.5	2.61 ± 0.05

4. Discussion

Recently, it has been shown that selective laser melted porous structures made from Ti6Al4V ELI and Ta can be clinically used as implant materials [17,24]. Although Ti6Al4V ELI is the current standard for load-bearing implant applications, Ta showed excellent *in vivo* performance and bone ingrowth. The ductile mechanical behavior and the high fatigue strength are believed to be one of the key factors for the performance of porous Ta implants, but due to high material cost, the use of Ta in large orthopedic implants is expected to remain relatively limited. In this study, the SLM technology was used to manufacture porous CP Ti structures based on dodecahedron unit cells with overall porosities ranging from 66% to 82% in order to compare them with previously published data of Ti6Al4V ELI and Ta structures with the same geometrical architecture.

A first part investigates whether CP Ti porous structures have similar static and dynamic mechanical properties as compared to pure Ta structures. It was observed that CP Ti porous structures continuously deform under increased compressive load, without reaching a first local maximum (Fig. 2A). This ductile mechanical behavior of CP Ti porous structures is very similar to what was previously reported for pure Ta [17]. In order to compare the actual measurable static mechanical properties, it is important to take the overall porosity into account. It was concluded that for both the yield strength and the plateau stress, there is no significant difference between the values of porous Ta and the trend lines of porous CP Ti obtained in this study (Fig. 2 C and D). To explain this resemblance, the properties of the solid pure metals Ta and CP Ti should be compared. Both metals are one phase metals, but they do have a different crystal structure; Ta has a cubic BCC structure and Ti has a close packed hexagonal HCP structure [39]. In terms of yield strength both Ta and CP Ti have similar bulk properties (Table 1). Since both metals are single phase ductile materials with similar yield strength, the resembling mechanical behavior of Ta and CP Ti as a porous structure can be explained. The stiffness of porous Ta does however appears to be different from the trend line of porous CP Ti stiffness values (Fig. 2 D). This difference can be explained by the fact that the stiffness of pure Ta is higher than that of CP Ti (Table 1). Regarding the dynamic mechanical

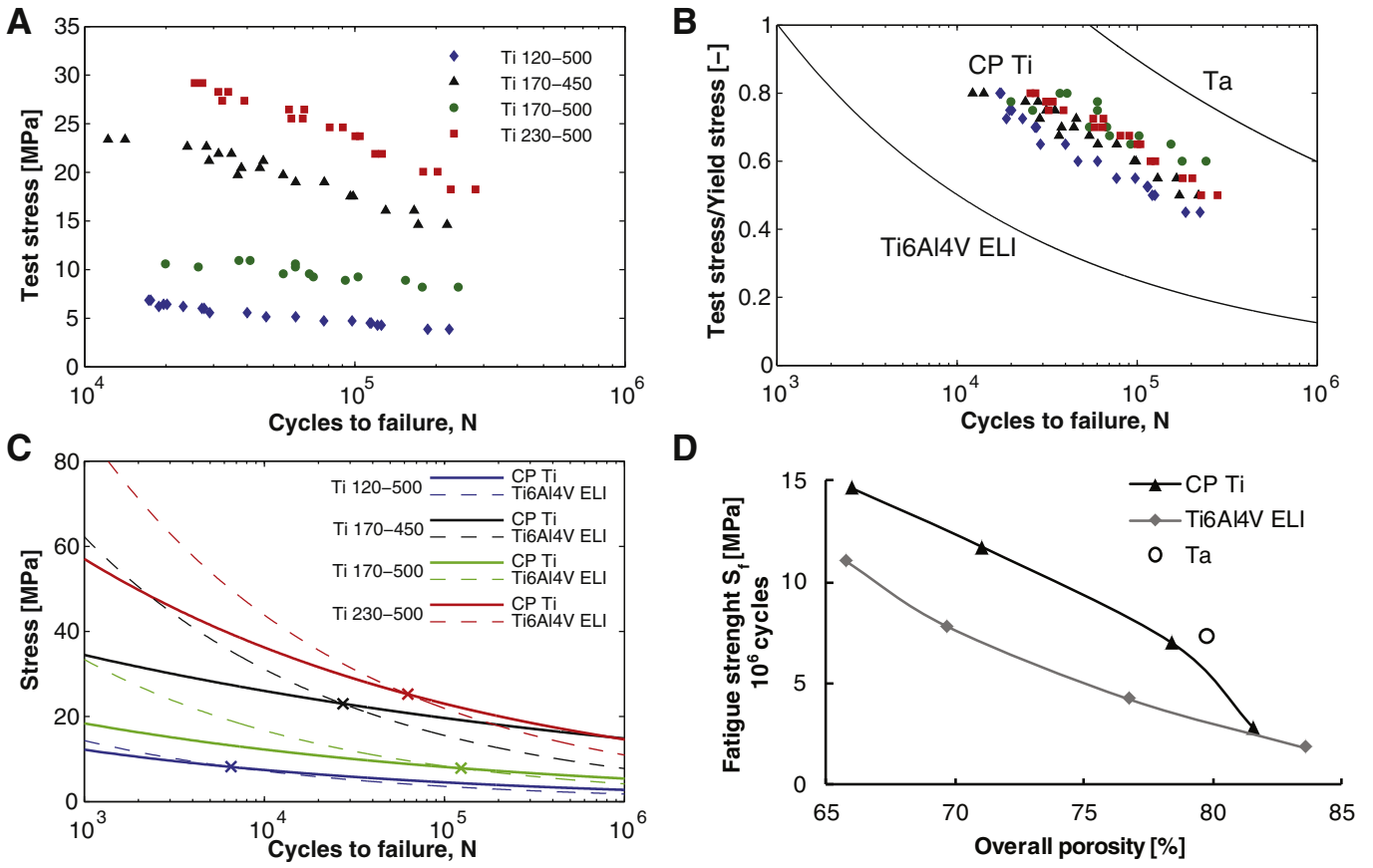

Fig. 3. Dynamic mechanical properties of open porous SLM processed titanium and tantalum structures: S-N curves obtained by compression-compression fatigue testing of all CP Ti samples using absolute (A) and normalized (B) stress values and a power law representing the results of Ti6Al4V ELI and Ta structures from previous studies (B) [17,23]; an overview of all fitted power laws for all four porous structures in both titanium materials using absolute stress values, including the structure intersection points marked by 'X' (C); an extrapolation of the fitted power laws to 10^6 cycles for all four porous structures in both titanium materials and the actual fatigue limit of the Ta structure versus the actual measured open porosity of each structure (D).

properties it was observed that porous Ta has a higher relative fatigue strength (0.58 σ_y vs. 0.41 σ_y) and since there is no significant difference in yield strength, this resulted in a slightly higher absolute fatigue strength for porous Ta compared to CP Ti (Fig. 3 D). In conclusion it can be stated that porous CP Ti has a comparable mechanical behavior compared to porous Ta, except that CP Ti has a slightly lower stiffness and absolute fatigue strength after 10^6 cycles. This is a very interesting finding, since in a previous study it was shown that the mechanical behavior of porous Ta was likely responsible for the excellent *in vivo* performance, which could now be replaced by the much cheaper, more commonly available and easier to process CP Ti. Therefore the authors suggest for future research to evaluate porous CP Ti implants in an *in vivo* animal study and compare the results with those obtained for porous Ta.

In the second part, identical porous structures in CP Ti and Ti6Al4V ELI have to be compared in order to understand their differences in static and dynamic mechanical properties. To do so, the researchers aimed to manufacture porous CP Ti structures with nearly identical geometrical properties as reported before for Ti6Al4V ELI [23]. The results show that the morphological properties of the CP Ti structures are very close to those of Ti6Al4V ELI, but nevertheless the small differences should be taken into account wherever possible because small changes in overall porosity can have significant influence on the mechanical properties. Firstly, comparing the mechanical behavior during compression testing already reveals a significant difference between both materials. While porous CP Ti continuously deforms during compression without fracture, Ti6Al4V ELI reaches a maximum compression point, after which the structure starts to fail locally. Due to the geometry of the Ti6Al4V ELI structure, non-failed parts of the structure continue to deform until they fail. This compressive failure behavior continues until a plateau is reached and full compression occurs. The difference in mechanical deformation or failure can also be seen on the test sample images after compression. The porous CP Ti sample is completely deformed (Fig. 2 A), whereas the Ti6Al4V ELI structure failed during compression testing (Fig. 2 B). This also explains the difference between the values of the plateau end e_{ple}, which occurs between 40 and 47 % strain for CP Ti and between 56 and 76% strain for Ti6Al4V ELI [23]. Because of the pure deformation of CP Ti structures, full or final compression occurs at lower strains. The yield strength is lower for CP Ti compared to Ti6Al4V ELI. This is also expected since the yield strength of wrought Ti6Al4V ELI is about four times the strength of CP Ti (Table 1). However, for the porous structures compared in this study, the Ti6Al4V ELI structures have a yield strength that is only 1.7 to 2.4 times more than that of CP Ti, as would be expected for standard grade 3 or 4 titanium, so the

Table 4
The power laws fitted to the data points of the normalized S-N curves for all four different series of porous CP Ti samples tested. When multiplied by the corresponding value of the yield strength, the power law of the absolute values is obtained. Also the extrapolated values at N = 10^6 cycles are listed.

Series	Fitted power law	R^2 value	Stress level at 10^6 cycles
Ti 120-500	$\sigma_y \cdot 6.266 \cdot N^{-0.215}$	0.98	0.32 σ_y
Ti 170-450	$\sigma_y \cdot 2.742 \cdot N^{-0.122}$	0.77	0.51 σ_y
Ti 170-500	$\sigma_y \cdot 4.465 \cdot N^{-0.177}$	0.93	0.39 σ_y
Ti 230-500	$\sigma_y \cdot 6.095 \cdot N^{-0.197}$	0.95	0.40 σ_y
All series	$\sigma_y \cdot 4.154 \cdot N^{-0.167}$	0.72	0.41 σ_y

reference values of wrought titanium do not hold true for SLM processed porous titanium. If, on the other hand, strength values of as-manufactured selective laser melted solid Ti6Al4V ELI (1110 MPa [47]) and CP Ti (555 MPa [48]) are used, it should be noted that SLM Ti6Al4V ELI is 40% and CP Ti is 170% stronger compared to their conventionally processed counterparts. By doing so, a yield strength ratio of 2.0 is obtained, which is closer to the values that were actually observed for both porous materials. The plateau stress is not significantly different in the range of 70-80% overall porosity, but it tends to be lower for CP Ti outside this interval. Also a strange curve in the trend line for CP Ti is noticeable for the Ti 170–450 series data point. Since this is the only series with smaller pore size compared to the others (450 μm vs. 500 μm) and since porous CP Ti continuously deforms as a whole instead of failing by local fracturing, it is assumed that these two factors are the reason for the particular curve in the trend line of the plateau stress of porous CP Ti. Given the ductile deformation behavior and the sensitivity of the plateau stress to the pore size, it is important to careful interpret and compare plateau stress for CP Ti, since the calculated values do not represent an actual plateau as is reached with Ti6Al4V ELI. The authors therefore suggest including the deformation mechanism for pure and ductile metals and corresponding definitions of representative values in a next revision of the ISO 13314 standard. The stiffness of porous CP Ti structures shows to be lower, but not significantly different for porosities >70%, compared to Ti6Al4 ELI. Since solid CP Ti has a lower stiffness compared to Ti6Al4V ELI (Table 1), and since both the overall porosity and deformation mechanism influence the stiffness of a cellular metal [49,50], the small differences for the porous structures in Fig. 2 D are justified. Summarizing the differences in static mechanical properties between porous CP Ti and Ti6Al4V ELI structures, it can be stated that selective laser melted porous CP Ti has about half the yield strength and a more ductile deformation mechanism compared to Ti6Al4V ELI, while the stiffness remains the same. When the normalized stress levels of the dynamic properties are compared, it can be concluded that CP Ti has a higher normalized fatigue strength, and an overall normalized fatigue strength after 10^6 cycles of 0.41 σ_y, which is 3.4 times higher than the normalized fatigue strength of Ti6Al4V ELI (Fig. 3 B, Table 4 and [23]). The S-N curves obtained by fitting power laws through all data series for absolute stress levels, reveal that the S-N curves of CP Ti and Ti6Al4V ELI for each separate series intersect at some point (Fig. 3 C). Keeping in mind that the porosities were not exactly the same for both materials, which will cause a shift in the intersection point of Ti 120–500 to the right and of Ti 170–500 to the left, it can be reasonably stated that all intersection points lie in the interval 10^4 – 10^5 cycles. Hence the general observation and conclusion is that Ti6Al4V ELI porous structures are mechanically stronger for static or low cycle fatigue (< 10^4 cycles) applications, whereas commercially pure CP Ti structures are mechanically superior for high cycle fatigue (> 10^5 cycles) applications. This statement is ratified by the extrapolated values at 10^6 cycles for both materials and for the full range of tested porosities, which show superior fatigue strength for porous CP Ti structures compared to Ti6Al4V ELI (Fig. 3 D). In general, titanium is known to have a very good fatigue resistance, and properties like crack initiation and crack propagation or growth are often used to explain or predict the fatigue behavior of a material. But for porous structures the situation is more complex, since it is a combination of actual material properties and the architectural properties of the structure itself. Assuming the structures do have identical geometrical morphology, it is reasonable to say that the ductile deformation behavior of porous CP Ti is likely to be the reason for the excellent high cycle fatigue performance, because ductile materials have a lower crack initiation and propagation by softening the material when loaded [51]. This, however, remains a remarkable observation since the wrought titanium alloys generally have a superior fatigue strength compared to commercially pure titanium grades (Table 1). Since little is known about the fatigue mechanism for porous metals in general and given that fatigue properties of additively manufactured solid Ti6Al4V ELI reported elsewhere are non-consistent [52–54], the authors consider it as future research to further investigate more in detail the fatigue behavior mechanism of porous metals manufactured by AM and how processing conditions (e.g. build direction) and post process heat treatments can influence these results. Heat treatments are often applied on parts made by SLM to reduce residual stresses in bulky parts or to improve the mechanical properties. The results discussed here are without any heat treatment and can change the static and dynamic properties of porous structures [55].

5. Conclusions

In this study the additive manufacturing technology selective laser melting was used to manufacture highly open porous (66-82%) CP grade 1 Ti structures. After a morphological characterization, both static and dynamic compression tests were done on four series of porous structures based on the dodecahedron unit cell architecture. The results were compared to previously reported data on identical porous structures in Ta [17] and Ti6Al4V ELI [23]. Based on the experimental results obtained in this study and the comparison with the other two already established orthopedic porous metals, it can be concluded that CP Ti is an excellent material for dynamically loaded porous implants. At first, it has almost identical mechanical behavior and properties compared to porous Ta, which has proven excellent *in vivo* performance, likely thanks to these properties. Secondly, for high cycle fatigue strength (> 10^5 cycles), CP Ti outperforms Ti6Al4V ELI, but for statically loaded or low cycle fatigue applications (<10^4 cycles), Ti6Al4V ELI remains the preferred material. These conclusions can have a potential huge impact on the medical device industry, because it brings CP Ti back in the scope of implant designers, has a lower cost compared to Ta and has the advantage of no potential hazardous or toxic alloying components like the presently applied titanium alloys. However, no comparative in vitro and *in vivo* data between additively manufactured CP Ti and Ti6Al4V ELI is available and the authors suggest to investigate this in future research.

Acknowledgements

This research was established by funding of the agency for Innovation by Science and Technology (IWT) of the Flemish government through Baekeland mandate 'IWT 100228'.

References

[1] J.A. Helsen, Y. Missirlis, Biomaterials - A Tantalus Experience, Springer, 2010.
[2] B.R. Levine, D.W. Fabi, Porous metals in orthopedic applications - A review (Poröse Metalle in orthopädischen Anwendungen - Eine Übersicht), Mater. Werkst. 41 (2010) 1001–1010.
[3] B. Levine, A New Era in Porous Metals: Applications in Orthopaedics, Adv. Eng. Mater. 10 (2008) 788–792.
[4] M.T. Andani, N.S. Moghaddam, C. Haberland, D. Dean, M.J. Miller, M. Elahinia, Metals for bone implants. Part 1. Powder metallurgy and implant rendering, Acta Biomater. 10 (10) (2014) 4058–4070.
[5] J.D. Bobyn, G.J. Stackpool, S.A. Hacking, M. Tanzer, J.J. Krygier, Characteristics of bone ingrowth and interface mechanics of a new porous tantalum biomaterial, J. Bone Joint Surg. Br. Vol. 81 (1999) 907–914.
[6] L.D. Zardiackas, D.E. Parsell, L.D. Dillon, D.W. Mitchell, L.A. Nunnery, R. Poggie, Structure, metallurgy, and mechanical properties of a porous tantalum foam, J. Biomed. Mater. Res. 58 (2001) 180–187.
[7] D.A. Shimko, V.F. Shimko, E.A. Sander, K.F. Dickson, E.A. Nauman, Effect of porosity on the fluid flow characteristics and mechanical properties of tantalum scaffolds, J. Biomed. Mater. Res. B Appl. Biomater. 73 (2005) 315–324.
[8] B.R. Levine, S. Sporer, R.A. Poggie, C.J. Della Valle, J.J. Jacobs, Experimental and clinical performance of porous tantalum in orthopedic surgery, Biomaterials 27 (2006) 4671–4681.
[9] B. Levine, C.J. Della Valle, J.J. Jacobs, Applications of porous tantalum in total hip arthroplasty, J. Am. Acad. Orthop. Surg. 14 (2006) 646–655.
[10] G. Lewis, Properties of open-cell porous metals and alloys for orthopaedic applications, J. Mater. Sci. Mater. Med. 24 (2013) 2293–2325.
[11] E. Marin, L. Fedrizzi, L. Zagra, Porous metallic structures for orthopaedic applications: a short review of materials and technologies, Eur. Orthop. Traumatol. 1 (2010) 103–109.
[12] B. Vandenbroucke, J.-P. Kruth, Selective laser melting of biocompatible metals for rapid manufacturing of medical parts, Rapid Prototyp. J. 13 (2007) 196–203.

[13] P. Heinl, L. Muller, C. Korner, R.F. Singer, F.A. Muller, Cellular Ti-6Al-4 V structures with interconnected macro porosity for bone implants fabricated by selective electron beam melting, Acta Biomater. 4 (2008) 1536–1544.
[14] J.P. Kruth, G. Levy, F. Klocke, T.H.C. Childs, Consolidation phenomena in laser and powder-bed based layered manufacturing, CIRP Ann. Manuf. Technol. 56 (2007) 730–759.
[15] G. Campoli, M.S. Borleffs, S. Amin Yavari, R. Wauthle, H. Weinans, A.A. Zadpoor, Mechanical properties of open-cell metallic biomaterials manufactured using additive manufacturing, Mater. Des. 49 (2013) 957–965.
[16] S.M. Ahmadi, G. Campoli, S. Amin Yavari, B. Sajadi, R. Wauthle, J. Schrooten, et al., Mechanical behavior of regular open-cell porous biomaterials made of diamond lattice unit cells, J. Mech. Behav. Biomed. Mater. 34C (2014) 106–115.
[17] R. Wauthle, J. van der Stok, S. Amin Yavari, J. Van Humbeeck, J.P. Kruth, A.A. Zadpoor, et al., Additively manufactured porous tantalum implants, Acta Biomater. 14 (2015) 217–225.
[18] C. Emmelmann, P. Scheinemann, M. Munsch, V. Seyda, Laser Additive Manufacturing of Modified Implant Surfaces with Osseointegrative Characteristics, Phys. Procedia 12 (2011) 375–384.
[19] S. Van Bael, G. Kerckhofs, M. Moesen, G. Pyka, J. Schrooten, J.P. Kruth, Micro-CT-based improvement of geometrical and mechanical controllability of selective laser melted Ti6Al4V porous structures, Mater. Sci. Eng. A 528 (2011) 7423–7431.
[20] S. Van Bael, Y.C. Chai, S. Truscello, M. Moesen, G. Kerckhofs, H. Van Oosterwyck, et al., The effect of pore geometry on the in vitro biological behavior of human periosteum-derived cells seeded on selective laser-melted Ti6Al4V bone scaffolds, Acta Biomater. 8 (2012) 2824–2834.
[21] G. Pyka, A. Burakowski, G. Kerckhofs, M. Moesen, S. Van Bael, J. Schrooten, et al., Surface Modification of Ti6Al4V Open Porous Structures Produced by Additive Manufacturing, Adv. Eng. Mater. 14 (2012) 363–370.
[22] J. Wieding, A. Jonitz, R. Bader, The Effect of Structural Design on Mechanical Properties and Cellular Response of Additive Manufactured Titanium Scaffolds, Materials 5 (2012) 1336–1347.
[23] S. Amin Yavari, R. Wauthle, J. van der Stok, A.C. Riemslag, M. Janssen, M. Mulier, et al., Fatigue behavior of porous biomaterials manufactured using selective laser melting, Mater. Sci. Eng., C 33 (2013) 4849–4858.
[24] J. van der Stok, H. Wang, S. Amin Yavari, M. Siebelt, M. Sandker, J.H. Waarsing, et al., Enhanced bone regeneration of cortical segmental bone defects using porous titanium scaffolds incorporated with colloidal gelatin gels for time- and dose-controlled delivery of dual growth factors, Tissue Eng. A 19 (2013) 2605–2614.
[25] J. Van der Stok, O.P. Van der Jagt, S. Amin Yavari, M.F. De Haas, J.H. Waarsing, H. Jahr, et al., Selective laser melting-produced porous titanium scaffolds regenerate bone in critical size cortical bone defects, J. Orthop. Res. 31 (2013) 792–799.
[26] S. Amin Yavari, J. van der Stok, Y.C. Chai, R. Wauthle, Z. Tahmasebi Birgani, P. Habibovic, et al., Bone regeneration performance of surface-treated porous titanium, Biomaterials 35 (2014) 6172–6181.
[27] F. Brenne, T. Niendorf, H.J. Maier, Additively manufactured cellular structures: Impact of microstructure and local strains on the monotonic and cyclic behavior under uniaxial and bending load, J. Mater. Process. Technol. 213 (2013) 1558–1564.
[28] E. Sallica-Leva, A.L. Jardini, J.B. Fogagnolo, Microstructure and mechanical behavior of porous Ti-6Al-4 V parts obtained by selective laser melting, J. Mech. Behav. Biomed. Mater. 26 (2013) 98–108.
[29] J. Sun, Y. Yang, D. Wang, Mechanical properties of a Ti6Al4V porous structure produced by selective laser melting, Mater. Des. 49 (2013) 545–552.
[30] V.J. Challis, X. Xu, L.C. Zhang, A.P. Roberts, J.F. Grotowski, T.B. Sercombe, High specific strength and stiffness structures produced using selective laser melting, Mater. Des. 63 (2014) 783–788.
[31] L.E. Murr, S.M. Gaytan, F. Medina, M.I. Lopez, E. Martinez, R.B. Wicker, Additive Layered Manufacturing of Reticulated Ti-6Al-4 V Biomedical Mesh Structures by Electron Beam Melting, in: A. McGoron, C.-Z. Li, W.-C. Lin (Eds.),25th Southern Biomedical Engineering Conference 2009, 15–17 May 2009, Springer Berlin Heidelberg, Miami, Florida, USA 2009, pp. 23–28.
[32] J. Parthasarathy, B. Starly, S. Raman, A. Christensen, Mechanical evaluation of porous titanium (Ti6Al4V) structures with electron beam melting (EBM), J. Mech. Behav. Biomed. Mater. 3 (2010) 249–259.
[33] S.J. Li, L.E. Murr, X.Y. Cheng, Z.B. Zhang, Y.L. Hao, R. Yang, et al., Compression fatigue behavior of Ti–6Al–4 V mesh arrays fabricated by electron beam melting, Acta Mater. 60 (2012) 793–802.
[34] X.Y. Cheng, S.J. Li, L.E. Murr, Z.B. Zhang, Y.L. Hao, R. Yang, et al., Compression deformation behavior of Ti-6Al-4 V alloy with cellular structures fabricated by electron beam melting, J. Mech. Behav. Biomed. Mater. 16 (2012) 153–162.
[35] T.J. Horn, O.L.A. Harrysson, D.J. Marcellin-Little, H.A. West, B.D.X. Lascelles, R. Aman, Flexural properties of Ti6Al4V rhombic dodecahedron open cellular structures fabricated with electron beam melting, Addit. Manuf. 1–4 (2014) 2–11.
[36] S.J. Li, Q.S. Xu, Z. Wang, W.T. Hou, Y.L. Hao, R. Yang, et al., Influence of cell shape on mechanical properties of Ti-6Al-4 V meshes fabricated by electron beam melting method, Acta Biomater. 10 (2014) 4537–4547.
[37] D.M. Brunette, P. Tengvall, M. Textos, P. Thomsen, Titanium in Medicine, Springer, Berlin Heidelberg, 2001.
[38] S. Lampman, Wrought Titanium and Titanium Alloys, Properties and Selection: Nonferrous Alloys and Special-Purpose Materials, ASM Handbook, ASM International 1990, pp. 592–633.
[39] W.S. Lyman, Properties of Pure Metals, Properties and Selection: Nonferrous Alloys and Special-Purpose Materials, ASM Handbook, ASM International 1990, p. 1099-201.
[40] L. Thijs, M.L. Montero Sistiaga, R. Wauthle, Q. Xie, J.-P. Kruth, J. Van Humbeeck, Strong morphological and crystallographic texture and resulting yield strength anisotropy in selective laser melted tantalum, Acta Mater. 61 (2013) 4657–4668.
[41] L. Mullen, R.C. Stamp, W.K. Brooks, E. Jones, C.J. Sutcliffe, Selective Laser Melting: a regular unit cell approach for the manufacture of porous, titanium, bone in-growth constructs, suitable for orthopedic applications, J. Biomed. Mater. Res. B Appl. Biomater. 89 (2009) 325–334.
[42] L. Mullen, R.C. Stamp, P. Fox, E. Jones, C. Ngo, C.J. Sutcliffe, Selective laser melting: a unit cell approach for the manufacture of porous, titanium, bone in-growth constructs, suitable for orthopedic applications. II. Randomized structures, J. Biomed. Mater. Res. B Appl. Biomater. 92 (2010) 178-88.
[43] A. Barbas, A.S. Bonnet, P. Lipinski, R. Pesci, G. Dubois, Development and mechanical characterization of porous titanium bone substitutes, J. Mech. Behav. Biomed. Mater. 9 (2012) 34–44.
[44] M. de Wild, R. Schumacher, K. Mayer, E. Schkommodau, D. Thoma, M. Bredell, et al., Bone regeneration by the osteoconductivity of porous titanium implants manufactured by selective laser melting: a histological and micro computed tomography study in the rabbit, Tissue Eng. A 19 (2013) 2645–2654.
[45] P. Lipinski, A. Barbas, A.S. Bonnet, Fatigue behavior of thin-walled grade 2 titanium samples processed by selective laser melting. Application to life prediction of porous titanium implants, J. Mech. Behav. Biomed. Mater. 28 (2013) 274–290.
[46] ISO 13314, Mechanical testing of metals – Ductility testing – Compression test for porous and cellular metals, 2011.
[47] B. Vrancken, L. Thijs, J.-P. Kruth, J. Van Humbeeck, Heat treatment of Ti6Al4V produced by Selective Laser Melting: Microstructure and mechanical properties, J. Alloys Compd. 541 (2012) 177–185.
[48] H. Attar, M. Calin, L.C. Zhang, S. Scudino, J. Eckert, Manufacture by selective laser melting and mechanical behavior of commercially pure titanium, Mater. Sci. Eng. A 593 (2014) 170–177.
[49] H.-P. Degischer, B. Kriszt, Handbook of Cellular Metals: Production, Processing, Applications, Wiley-VCH Verlag GmbH & Co. KGaA, 2002.
[50] L.J. Gibson, M.F. Ashby, Cellular Solids - Structure and Properties, Cambridge University Press, 1999.
[51] R.O. Ritchie, Mechanisms of fatigue-crack propagation in ductile and brittle solids, Int. J. Fract. 100 (1999) 55–83.
[52] K.S. Chan, M. Koike, R.L. Mason, T. Okabe, Fatigue Life of Titanium Alloys Fabricated by Additive Layer Manufacturing Techniques for Dental Implants, Metall. Mater. Trans. A 44 (2012) 1010–1022.
[53] S. Leuders, M. Thöne, A. Riemer, T. Niendorf, T. Tröster, H.A. Richard, et al., On the mechanical behaviour of titanium alloy TiAl6V4 manufactured by selective laser melting: Fatigue resistance and crack growth performance, Int. J. Fatigue 48 (2013) 300–307.
[54] P. Edwards, M. Ramulu, Fatigue performance evaluation of selective laser melted Ti–6Al–4 V, Mater. Sci. Eng. A 598 (2014) 327–337.
[55] R. Wauthle, B. Vrancken, B. Beynaerts, K. Jorissen, J. Schrooten, J.-P. Kruth, et al., Effects of build orientation and heat treatment on the microstructure and mechanical properties of selective laser melted Ti6Al4V lattice structures, Addit. Manuf. 5 (2015) 77–84.